

Electronic Supplementary Information for

Efficient Electrochemiluminescence of a Readily Accessible Boron Difluoride Formazanate Dye

Mahdi Hesari, Stephanie M. Barbon, Viktor N. Staroverov, Zhifeng Ding*,
and Joe B. Gilroy*

E-mails: zfding@uwo.ca , joe.gilroy@uwo.ca

Department of Chemistry and the Centre for Advanced Materials and Biomaterials Research
(CAMBR), The University of Western Ontario, London, Ontario, Canada, N6A 5B7.

Table of Contents

Experimental Details.....	S2
Additional Figures.....	S6
Computational Details.....	S15
References.....	S22

Experimental Details

Synthetic Procedures

Boron difluoride formazanate dye **2a** was prepared according to a previously published protocol.¹

Electrochemistry and ECL Measurements

The electrochemical and ECL studies of dye **2a** were carried out using a 2 mm diameter Pt disc inlaid in a glass sheath as the working electrode (WE), a coiled Pt wire as the counter electrode (CE), and a coiled Pt wire as the quasi-reference electrode (QRE). After each experiment, the electrochemical potential window was calibrated using ferrocene as the internal standard. The redox potential of the ferrocene/ferrocenium (Fc/Fc⁺) couple was taken as 0.40 V vs. SCE.² In annihilation ECL studies, a solution containing approximately 0.1 mM of dye **2a**, 0.1 M *n*Bu₄NPF₆ as the supporting electrolyte and 3.0 mL anhydrous acetonitrile was added to the electrochemical cell with a flat Pyrex window at the bottom for detection of generated ECL, which was assembled in a glove box. For co-reactant studies, 20 mM tri-*n*-propylamine was added to the annihilation solution and the air-tight cell was assembled in a glove box.

Cyclic voltammetry experiments were performed using a CHI 610A electrochemical analyzer (CH Instruments, Austin, TX). The general experimental parameters for the cyclic voltammetry experiments were as follows: 0.000 V initial potential in experimental scale, positive or negative initial scan polarity, 0.1 V s⁻¹ scan rate, 4 sweep segments, 0.001 V sample interval, 2 s quiet time, 1.5 × 10⁻⁵ AV⁻¹ sensitivity. The differential pulse voltammograms (DPVs, Fig. S1) were obtained with a pulse amplitude of 0.05 V, pulse width of 0.05 s, increment of 2 mV per cycle, pulse period of 0.2 s, and quiet time of 2 s.

The ECL-voltage curves were obtained using the CHI 610A coupled with a photomultiplier tube (PMT, R928, Hamamatsu, Japan) held at -750 V with a high voltage power supply. The ECL was collected by the PMT under the flat Pyrex window at the bottom of the cell, and was measured as a photocurrent before it was transformed to a voltage signal using a picoammeter/voltage source (Keithley 6487, Cleveland, OH). The potential and current signals from the electrochemical workstation and the photocurrent signal from the picoammeter were sent simultaneously through a DAQ board (DAQ 6052E, National Instruments, Austin, TX) to a

computer. The data acquisition system was controlled from a custom-made LabVIEW program (ECL_PMT610a.vi, National Instruments, Austin, TX). The photosensitivity on the picoammeter was set manually in order to avoid signal saturation. ECL spectroscopy was conducted on an Acton 2300i spectrograph with two gratings (50 l/mm blazed at 600 nm and 300 l/mm blazed at 700 nm) and an Andor iDUS CCD camera (Model DU401-BR-DD-352). The spectrograph and camera were calibrated using a mercury lamp each time. The accumulated ECL spectra were recorded during two successive potential scan cycles. The spooling ECL spectra were recorded using the Andor Technology program during a potential scan cycle. The following parameters were used for the Andor Technology program under the kinetic parameters option tab: exposure time = 1 s, number of accumulations = 1, kinetic series length = 200 s to match with the potential scan cycle between 0.2 and 2.2 V at a scan rate of 20 mV/s, kinetic cycle time = 1 s, and the spectrometer was centred at 700 nm using the 50 l/mm grating. In other words, if the potential scan window is 1 V and the scan rate is 100 mV/s, then the kinetic series length will be 10 s and 10 individual spectra will be collected.

Photoluminescence Spectroscopy

Photoluminescence spectra were acquired from a 1 μ M solution of **2a** using the same CCD camera and Acton spectrograph set with a 532 nm wavelength laser. A long-pass edge filter was placed between the sample and the spectrograph entrance to cut the excitation wavelength and harmonic peaks.

ECL Efficiency Calculations

As an example, ECL efficiency values were calculated by integrating ECL intensities *vs.* time and the corresponding cyclic voltammogram *vs.* time, and comparing the integrated ECL intensities (equivalent to the number of photons generated) and the current values (equivalent to the number of charges) of the **2a**/TPrA samples with those of the reference Ru(bpy)₃²⁺/TPrA during the ECL experiments. The quantum yield was calculated using the below equation:

$$\Phi_x = 100x \left(\frac{\int_a^b ECL dt}{\int_a^b Current dt} \right)_x / \left(\frac{\int_a^b ECL dt}{\int_a^b Current dt} \right)_{St}$$

where Φ is the quantum yield (%) relative to the Ru(bpy)₃²⁺/TPrA,³ ECL is the ECL intensity,

current is the electrochemical current value, St is the standard [Ru(bpy)₃²⁺/TPrA] and x is the sample (**2a** /TPrA).

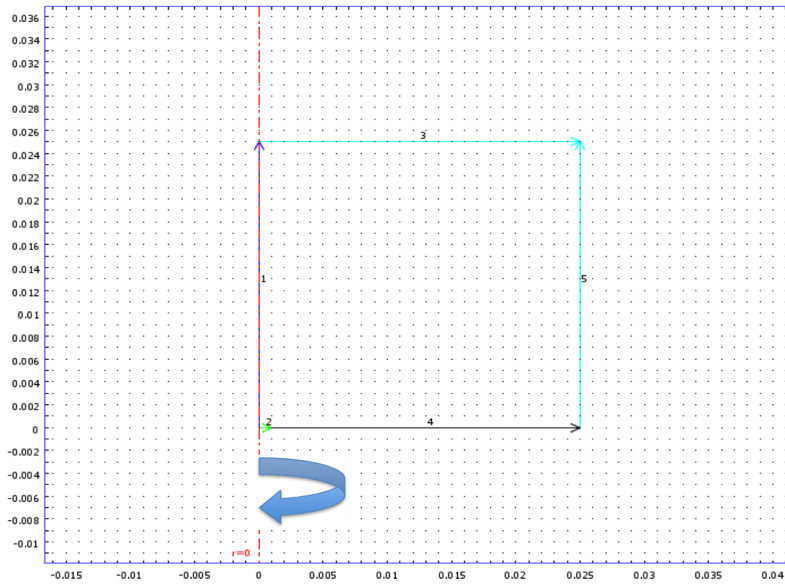
COMSOL Simulations

The simulated geometry shown below was composed of 5 boundaries enclosing a domain within which mass transfer was described by Fick's laws of diffusion through equation 1:⁴

$$\frac{\partial c_{i,\alpha}(r, z, t)}{\partial t} = D_{i,\alpha} \left(\frac{\partial^2 c_{i,\alpha}(r, z, t)}{\partial r^2} + \frac{1}{r} \frac{\partial c_{i,\alpha}(r, z, t)}{\partial r} + \frac{\partial^2 c_{i,\alpha}(r, z, t)}{\partial z^2} \right) \quad (1)$$

$$= D_{i,\alpha} \nabla c_{i,\alpha}(r, z, t) = 0$$

where $c_{i,\alpha}$ and $D_{i,\alpha}$ are the concentration and diffusion coefficients of redox species i in solution α , ∇ , or del, is the gradient or vector operator – shown here in cylindrical coordinates.



The box describes the simplified simulation domain with boundaries 1, 2, 3, 4, and 5 defined as axial symmetry, the electrode surface, concentration, glass insulator, and concentration, respectively.

The simple one-electron oxidation/reduction reaction, as defined by equation 2, and operated at the electrode surface via boundary 2:



where the reduced species, Red, is oxidized to Ox through loss of one electron, e^- . The reaction kinetics were assumed to follow the Butler-Volmer regime represented by equations 3 and 4 for the forward (k_f) and reverse (k_b) rates:⁵

$$k_f = k^o \exp\left(-\gamma f (E - E^{o'})\right) \quad (3)$$

$$k_b = k^o \exp\left((1 - \gamma) f (E - E^{o'})\right) \quad (4)$$

Here k^o is the standard rate constant, γ is the transfer coefficient (this was assumed to be 0.5 unless otherwise stated), and $f = F/(RT)$; F is Faraday's constant, R is the universal gas constant, and T is temperature in Kelvin (assumed to be room temperature, 298.15 K or 25 °C). E is the applied potential scanned between 1 and 2 V at a scan rate of 20 mV/s and $E^{o'}$ the formal redox potential (1.8 V).

The other boundary conditions were set as axial symmetry, concentration, insulator, and concentration for 1, 3, 4, and 5, respectively. The initial concentration of the oxidized form, $[\text{Ox}]_{\text{initial}}$, was set to zero unless otherwise stated, while $[\text{Red}]_{\text{initial}} = 1 \text{ mM}$; this corresponds to the initial experimental conditions where, for example, **2a** is the reduced form and is oxidized to **2a⁺**. Three cases were simulated in Figure S2: (A) simple reversible electrochemical reaction of **2a**; (B) electrochemical reaction followed by a chemical reaction of Ox, **2a⁺**; and (C) electrochemical reaction followed by a chemical reaction of **2a⁺** in the vicinity of the electrode with **2a** in the surrounding solution, and some **2a⁺** undergoing a decomposition reaction. Detailed COMSOL codes and their model reports are available upon request.

In Figure S2C, the anodic current is enhanced, as observed experimentally for the oxidation of **2a** (Fig. 1 and Fig. S1), while the cathodic current is small. The simulation agrees well with our proposition on the first oxidation process.

Additional Figures

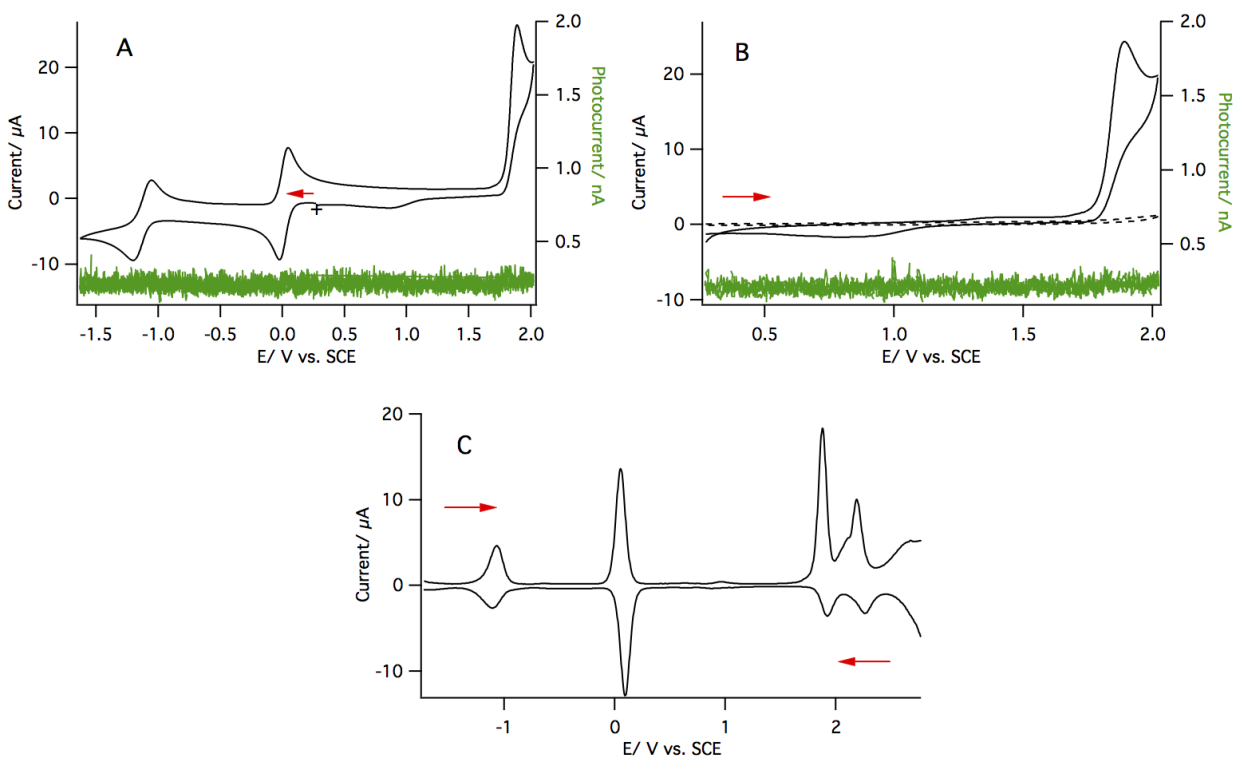


Fig. S1 Cyclic voltammograms (A, B) and differential pulse voltammograms (C) of a 0.1 mM acetonitrile solution of **2a** containing 0.1 M *n*Bu₄NPF₆ at a scan rate of 100 mV s⁻¹. The arrow and cross show the direction and starting potential of the scan. The first oxidation reaction is unlikely to involve a two-electron process based on the DPV data as the anodic peak heights for the first reduction and oxidation are similar.

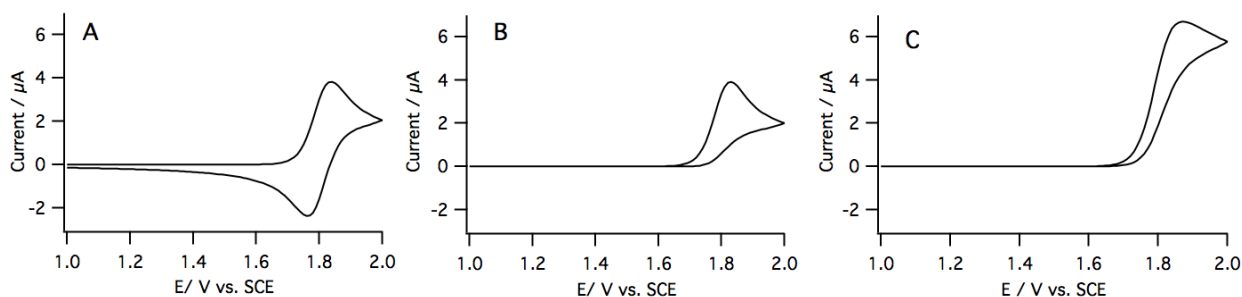


Fig. S2 Simulated cyclic voltammograms of (A) simple reversible electrochemical reaction of **2a**; (B) electrochemical reaction followed by a chemical reaction of the oxidized species, **2a**^{•+}; and (C) electrochemical reaction followed by a chemical reaction of **2a**^{•+} in the vicinity of the electrode with **2a** in the surrounding solution, with some **2a**^{•+} undergoing a decomposition reaction.

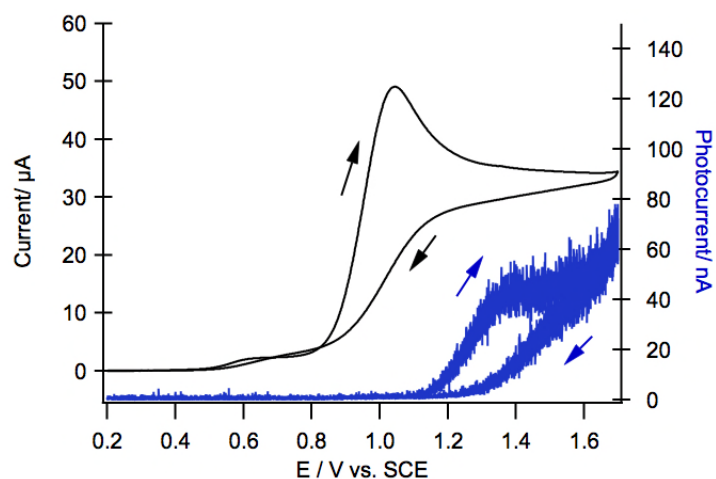


Fig. S3 ECL-voltage curve (blue) and the corresponding cyclic voltammogram of a 0.1 mM acetonitrile solution of **2a** in the presence of 20 mM TPrA and 0.1 M *n*Bu₄NPF₆ at a scan rate of 20 mV s⁻¹ in the potential range of 0.2 to 1.7 V vs. SCE.

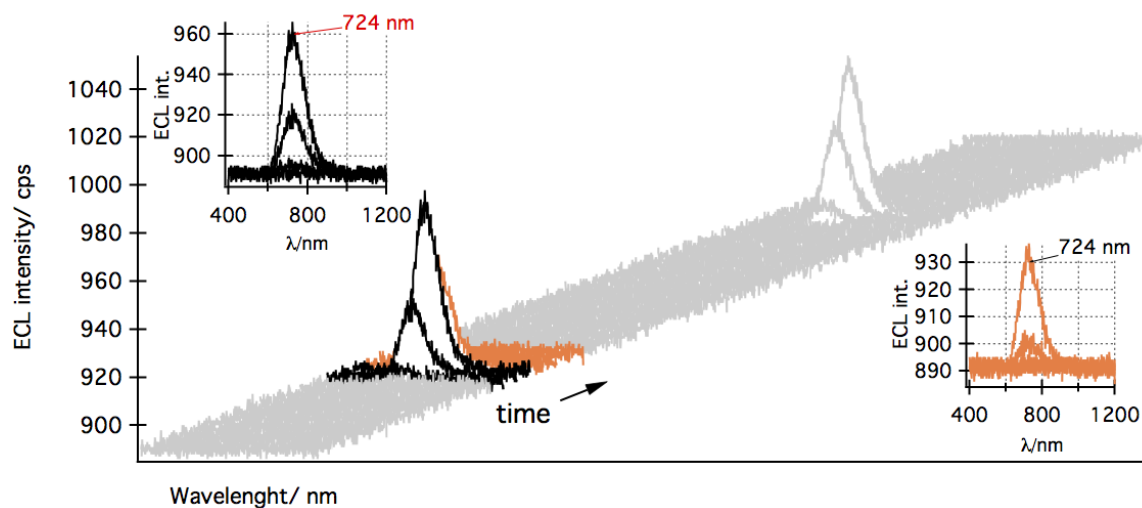


Fig. S4 Spooling ECL spectra of a 0.1 mM acetonitrile solution of **2a** in the presence of 20 mM TPrA and 0.1 M *n*Bu₄NPF₆ at a scan rate of 20 mV s⁻¹. The insets show the stacked spectra for ECL emission evolution (the black spectra) and devolution (the orange spectra). All spectra were recorded for 1 s in two consecutive potential scan cycles from 0.2 to 1.7 V vs. SCE. The spooling spectra were collected between 400 and 1200 nm.

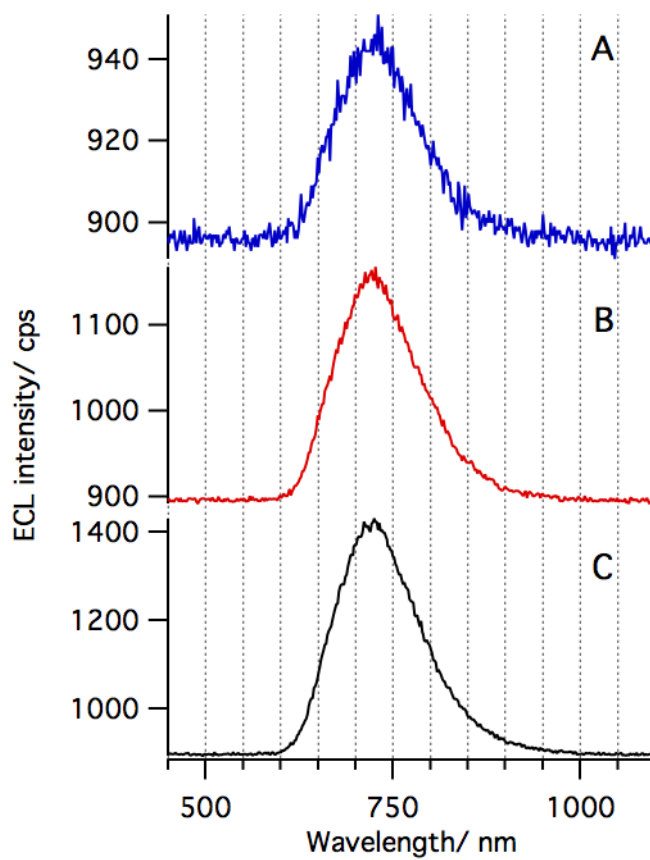


Fig. S5 Selected spooling ECL spectra of a 0.1 mM acetonitrile solution of **2a** in the presence of 20 mM TPrA and 0.1 M *n*Bu₄NPF₆ at various potentials: (A) at 1.5 V, (B) 1.86 V, and (C) 1.98 V (reverse scan).

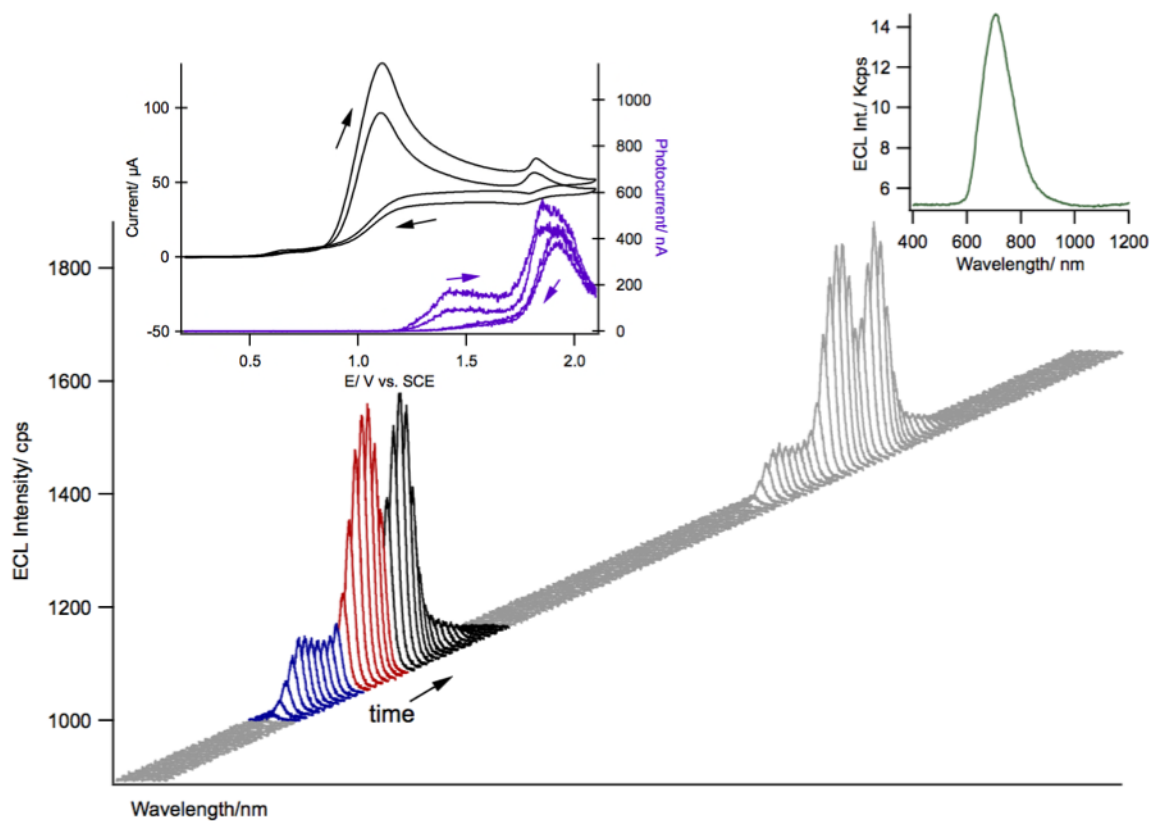


Fig. S6 Spooling ECL spectra of an acetonitrile solution containing 0.1 mM **2a** in the presence of 20 mM TPrA and 0.1 M $n\text{Bu}_4\text{NPF}_6$ at a scan rate of 50 mV s^{-1} . The insets show the related ECL-voltage curve (purple) and the corresponding cyclic voltammograms (top left panel) and accumulated ECL spectrum (top right panel). All spectra were recorded for 1 s in two consecutive potential scan cycles from 0.2 to 2.1 V vs. SCE. The spooling spectra were collected between 400 and 1200 nm.

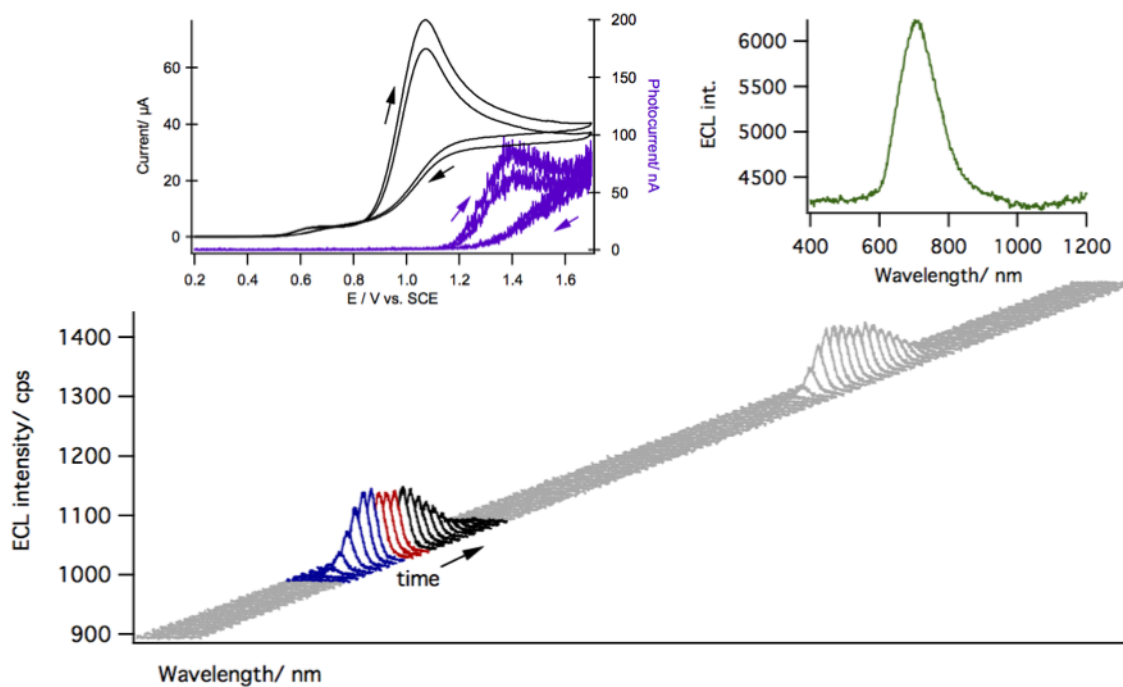


Fig. S7 Spooling ECL spectra of an acetonitrile solution containing 0.1 mM **2a** in the presence of 20 mM TPrA and 0.1 M $n\text{Bu}_4\text{NPF}_6$ at a scan rate of 50 mV s^{-1} . The insets show the related ECL-voltage curve (purple) and the corresponding cyclic voltammograms (top left panel) and accumulated ECL spectrum (top right panel). All spectra were recorded for 1 s in two consecutive potential scan cycles from 0.2 to 1.7 V vs. SCE. The spooling spectra were collected between 400 and 1200 nm.

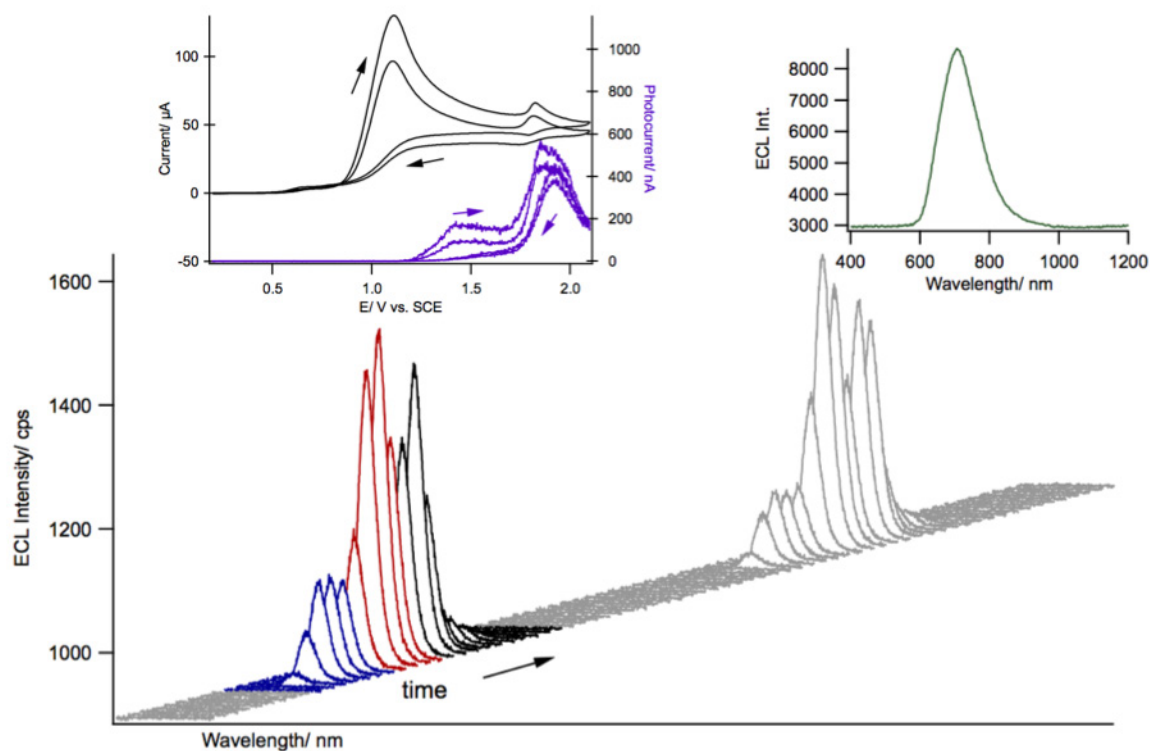


Fig. S8 Spooling ECL spectra of an acetonitrile solution containing 0.1 mM **2a** in the presence of 20 mM TPrA and 0.1 M $n\text{Bu}_4\text{NPF}_6$ at a scan rate of 100 mV s^{-1} . The insets show the related ECL-voltage curve (purple) and the corresponding cyclic voltammograms (top left panel) and accumulated ECL spectrum (top right panel). All spectra were recorded for 1 s in two consecutive potential scan cycles from 0.2 to 2.1 V vs. SCE. The spooling spectra were between from 400 and 1200 nm.

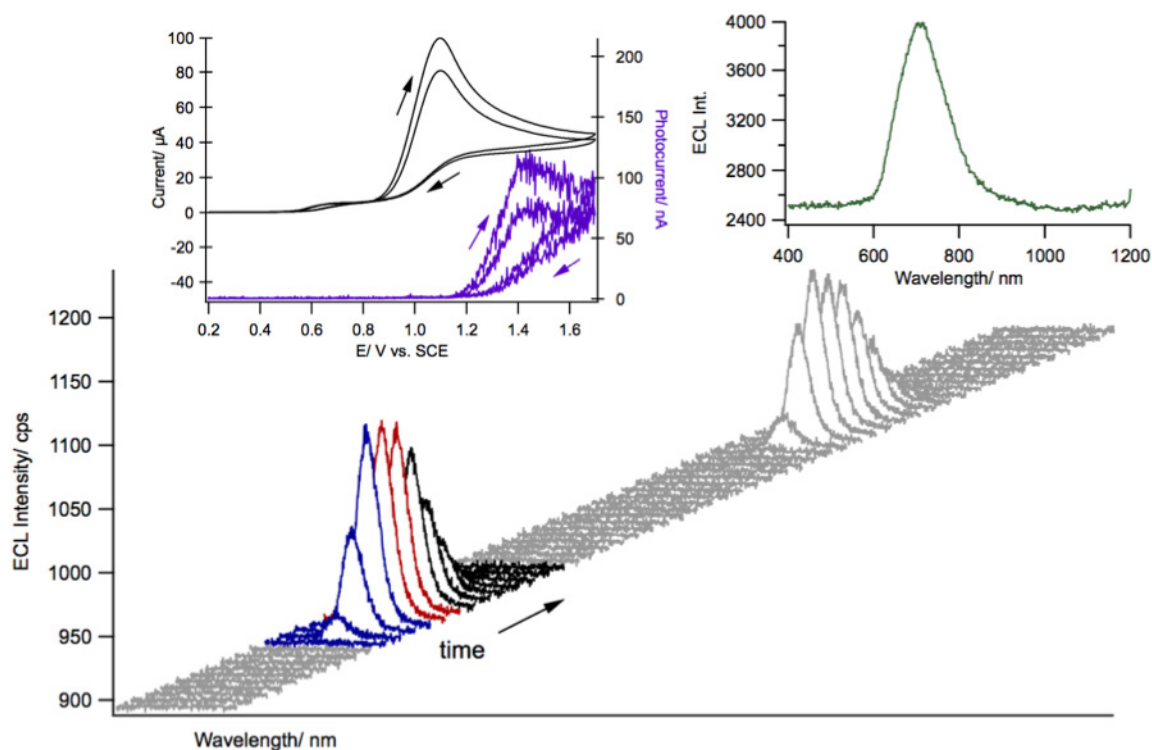


Fig. S9 Spooling ECL spectra of an acetonitrile solution containing 0.1 mM **2a** in the presence of 20 mM TPrA and 0.1 M $n\text{Bu}_4\text{NPF}_6$ at a scan rate of 100 mV s^{-1} . The insets show the related ECL-voltage curve (purple) and the corresponding cyclic voltammograms (top left panel) and accumulated ECL spectrum (top right panel). All spectra were recorded for 1 s in two consecutive potential scan cycles from 0.2 to 1.7 V vs. SCE. The spooling spectra were collected between 400 and 1200 nm.

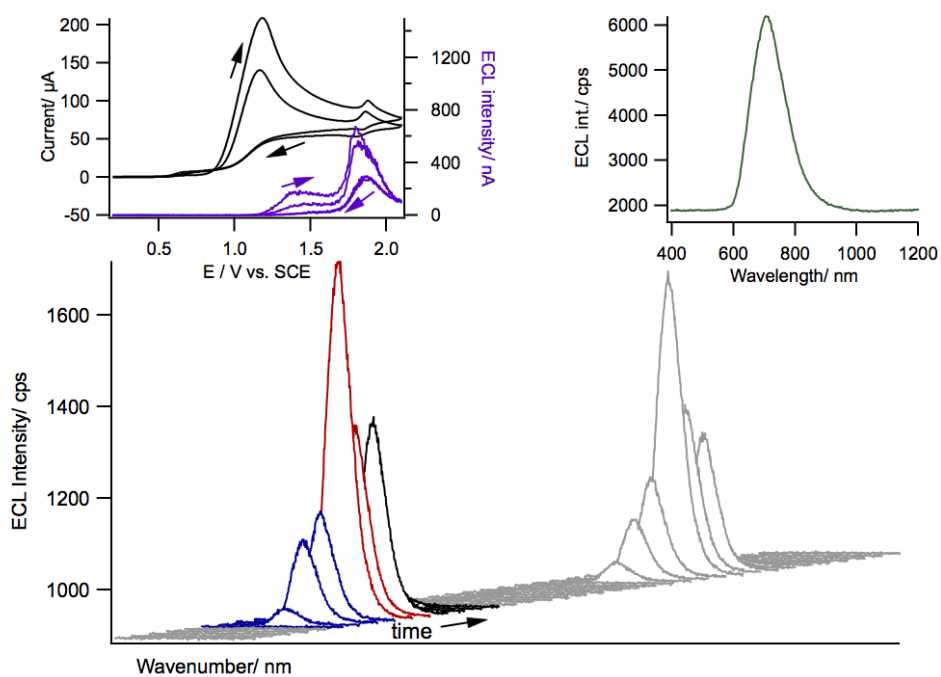


Fig. S10 Spooling ECL spectra of an acetonitrile solution containing 0.1 mM **2a** in the presence of 20 mM TPrA and 0.1 M *n*Bu₄NPF₆ at a scan rate of 200 mV s⁻¹. The insets show the related ECL-voltage curve (purple) and the corresponding cyclic voltammograms (top left panel) and accumulated ECL spectrum (top right panel). All spectra were recorded for 1 s in two consecutive potential scan cycles from 0.2 to 2.1 V vs. SCE. The spooling spectra were collected between 400 and 1200 nm.

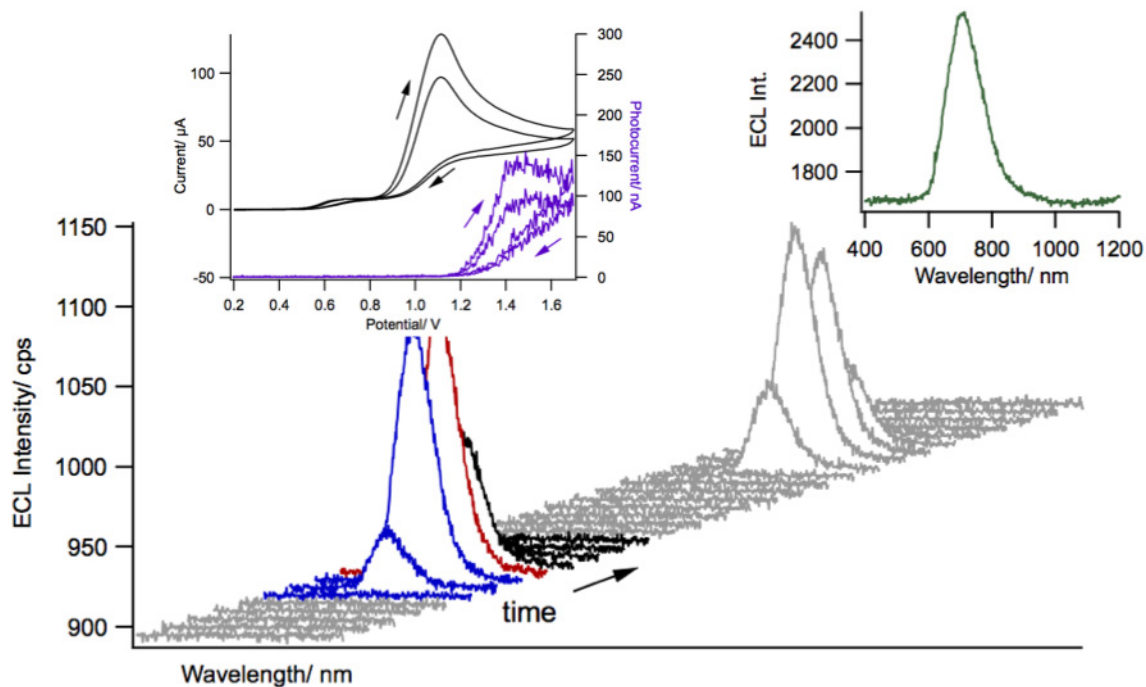
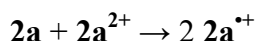


Fig. S11 Spooling ECL spectra of an acetonitrile solution containing 0.1 mM **2a** in the presence of 20 mM TPrA and 0.1 M $n\text{Bu}_4\text{NPF}_6$ at a scan rate of 200 mV s^{-1} . The insets show the related ECL-voltage curve (purple) and the corresponding cyclic voltammograms (top left panel) and accumulated ECL spectrum (top right panel). All spectra were recorded for 1 s in two consecutive potential scan cycles from 0.2 to 1.7 V vs. SCE. The spooling spectra were collected between 400 and 1200 nm.

Computational Details

The thermodynamics of the comproportionation reaction



was studied computationally in vacuum and in acetonitrile solution using the *Gaussian 09* program.⁶

Methodology. Molecular geometries of the three species involved were optimized using the ω B97X-D functional,⁷ which includes an empirical dispersion correction, and the 6-311+G* basis set. The UltraFine integration grid was employed in all calculations. Solvation effects were treated implicitly using the polarizable continuum model (PCM). The calculations for the radical cation ($\mathbf{2a}^{\bullet+}$) were spin-unrestricted. All optimized structures were verified by vibrational analysis to be minima on the potential energy surface. The optimized structures for $\mathbf{2a}$, $\mathbf{2a}^{\bullet+}$, and $\mathbf{2a}^{2+}$ were found by unconstrained search to have the C_s , C_{2v} , and C_{2v} symmetries, respectively. The Cartesian coordinates of the optimized structures (cleaned up by re-optimizing them under the corresponding symmetry constraints) are reported below.

Results

Table S1. Calculated ω B97X-D/6-311+G* energies of $\mathbf{2a}$, $\mathbf{2a}^{\bullet+}$, and $\mathbf{2a}^{2+}$. E_e is the total electronic energy, E_0 is the sum of the total electronic energy and the zero-point energy, G°_{298} is the standard Gibbs free energy at 298 K. All values are in hartree units (1 hartree = 2625.5 kJ mol⁻¹).

Property	$\mathbf{2a}$	$\mathbf{2a}^{\bullet+}$	$\mathbf{2a}^{2+}$
Vacuum			
E_e	-1266.832685	-1266.561667	-1266.162206
E_0	-1266.535639	-1266.265054	-1265.864456
G°_{298}	-1266.589538	-1266.318723	-1265.917354
Acetonitrile solution			
E_e	-1266.850128	-1266.627292	-1266.378192
E_0	-1266.553253	-1266.331238	-1266.081150
G°_{298}	-1266.606632	-1266.385211	-1266.136512

Table S2. Reaction energies (in kJ mol⁻¹) calculated at the ω B97X-D/6-311+G* level of theory.

Property	Vacuum	Acetonitrile solution
ΔE_e	-337.2	-69.0
ΔE_0	-341.3	-73.7
ΔG°_{298}	-342.8	-71.6

Table S3. Optimized ω B97X-D/6-311+G* structures of **2a**, **2a⁺**, **2a²⁺** given in the *Gaussian 09* format. All coordinates are in Å.

```

# wB97XD/6-311+G* Int(Grid=UltraFine)
Neutral 2a, wB97X-D/6-311+G* structure (Cs) in vacuum
0,1
C    -0.977700    0.669090    2.853686
C     0.194754    0.014217    2.500553
C     0.787076   -0.887099    3.387739
C     0.209111   -1.122797    4.616179
C    -0.970984   -0.464478    4.979475
C    -1.561557    0.434165    4.091306
N     0.797033    0.274025    1.235658
B    -0.061166    0.708032    0.000000
F    -0.205998    2.090809    0.000000
O    -1.459909   -0.766288    6.200038
C    -2.653876   -0.142224    6.622901
N     2.071479    0.166416    1.194391
C     2.669862    0.217796    0.000000
C     4.101763    0.149546    0.000000
N     5.251389    0.105290    0.000000
N     2.071479    0.166416   -1.194391
N     0.797033    0.274025   -1.235658
C     0.194754    0.014217   -2.500553
C     0.787076   -0.887099   -3.387739
C     0.209111   -1.122797   -4.616179
C    -0.970984   -0.464478   -4.979475
C    -1.561557    0.434165   -4.091306
C    -0.977700    0.669090   -2.853686
O    -1.459909   -0.766288   -6.200038
C    -2.653876   -0.142224   -6.622901
F    -1.274203    0.056197    0.000000
H     1.697859   -1.400678   -3.105082
H     0.650139   -1.824093   -5.314776
H    -2.470872    0.962583   -4.346933
H    -1.435714    1.378665   -2.176747
H     1.697859   -1.400678    3.105082
H     0.650139   -1.824093    5.314776
H    -2.470872    0.962583    4.346933
H    -1.435714    1.378665    2.176747
H    -2.859220   -0.533608    7.617074
H    -2.536109    0.944908    6.679759
H    -3.488244   -0.387951    5.957754
H    -2.859220   -0.533608   -7.617074
H    -3.488244   -0.387951   -5.957754
H    -2.536109    0.944908   -6.679759

```

--link1--

wB97XD/6-311+G* Int(Grid=UltraFine)

Cation 2a(+), wB97X-D/6-311+G* structure (C2v) in vacuum

1,2

C	0.000000	2.730277	-1.189435
C	0.000000	2.546743	0.216435
C	0.000000	3.688447	1.065857
C	0.000000	4.938257	0.529162
C	0.000000	5.116299	-0.878347
C	0.000000	3.990081	-1.727912
N	0.000000	1.278813	0.749429
B	0.000000	0.000000	-0.193527
F	1.151519	0.000000	-0.946641
O	0.000000	6.363558	-1.290577
C	0.000000	6.669196	-2.687752
N	0.000000	1.207198	2.051104
C	0.000000	0.000000	2.613572
C	0.000000	0.000000	4.050530
N	0.000000	0.000000	5.200072
N	0.000000	-1.207198	2.051104
N	0.000000	-1.278813	0.749429
C	0.000000	-2.546743	0.216435
C	0.000000	-3.688447	1.065857
C	0.000000	-4.938257	0.529162
C	0.000000	-5.116299	-0.878347
C	0.000000	-3.990081	-1.727912
C	0.000000	-2.730277	-1.189435
O	0.000000	-6.363558	-1.290577
C	0.000000	-6.669196	-2.687752
F	-1.151519	0.000000	-0.946641
H	0.000000	-3.553155	2.138370
H	0.000000	-5.820661	1.157438
H	0.000000	-4.104081	-2.803690
H	0.000000	-1.880096	-1.855548
H	0.000000	3.553155	2.138370
H	0.000000	5.820661	1.157438
H	0.000000	4.104081	-2.803690
H	0.000000	1.880096	-1.855548
H	0.000000	7.753570	-2.744127
H	0.898914	6.273218	-3.164291
H	-0.898914	6.273218	-3.164291
H	0.000000	-7.753570	-2.744127
H	-0.898914	-6.273218	-3.164291
H	0.898914	-6.273218	-3.164291

--link1--

wB97XD/6-311+G* Int(Grid=UltraFine)

Dication 2a(2+), wB97X-D/6-311+G* structure (C2v) in vacuum

2,1

C	0.000000	2.725461	-1.217699
C	0.000000	2.531975	0.215869
C	0.000000	3.690271	1.084422
C	0.000000	4.929582	0.557458
C	0.000000	5.109142	-0.869971
C	0.000000	3.971704	-1.743686
N	0.000000	1.300911	0.731525
B	0.000000	0.000000	-0.220737
F	1.154524	0.000000	-0.946074
O	0.000000	6.325997	-1.267493
C	0.000000	6.705707	-2.668879
N	0.000000	1.216401	2.048008
C	0.000000	0.000000	2.585300
C	0.000000	0.000000	4.022235
N	0.000000	0.000000	5.171826
N	0.000000	-1.216401	2.048008
N	0.000000	-1.300911	0.731525
C	0.000000	-2.531975	0.215869
C	0.000000	-3.690271	1.084422
C	0.000000	-4.929582	0.557458
C	0.000000	-5.109142	-0.869971
C	0.000000	-3.971704	-1.743686
C	0.000000	-2.725461	-1.217699
O	0.000000	-6.325997	-1.267493
C	0.000000	-6.705707	-2.668879
F	-1.154524	0.000000	-0.946074
H	0.000000	-3.542103	2.155526
H	0.000000	-5.816852	1.179362
H	0.000000	-4.105181	-2.817523
H	0.000000	-1.875214	-1.884523
H	0.000000	3.542103	2.155526
H	0.000000	5.816852	1.179362
H	0.000000	4.105181	-2.817523
H	0.000000	1.875214	-1.884523
H	0.000000	7.790368	-2.658362
H	0.903624	6.328340	-3.146920
H	-0.903624	6.328340	-3.146920
H	0.000000	-7.790368	-2.658362
H	-0.903624	-6.328340	-3.146920
H	0.903624	-6.328340	-3.146920

--link1--

wB97XD/6-311+G* Int(Grid=UltraFine)
SCRF=(PCM,Solvent=Acetonitrile)

Neutral 2a, wB97X-D/6-311+G* structure (Cs) in acetonitrile

0,1

C	-0.921320	0.746700	2.886281
C	0.194723	0.020665	2.488261
C	0.717257	-0.974873	3.316306
C	0.127323	-1.230950	4.535983
C	-0.994241	-0.499313	4.946717
C	-1.516763	0.492662	4.114080
N	0.810627	0.300194	1.234420
B	-0.027254	0.763157	0.000000
F	-0.124910	2.155220	0.000000
O	-1.500432	-0.825194	6.151622
C	-2.646890	-0.129710	6.618857
N	2.082303	0.169114	1.195471
C	2.678807	0.216594	0.000000
C	4.108295	0.126835	0.000000
N	5.257854	0.069901	0.000000
N	2.082303	0.169114	-1.195471
N	0.810627	0.300194	-1.234420
C	0.194723	0.020665	-2.488261
C	0.717257	-0.974873	-3.316306
C	0.127323	-1.230950	-4.535983
C	-0.994241	-0.499313	-4.946717
C	-1.516763	0.492662	-4.114080
C	-0.921320	0.746700	-2.886281
O	-1.500432	-0.825194	-6.151622
C	-2.646890	-0.129710	-6.618857
F	-1.269970	0.162368	0.000000
H	1.575329	-1.552235	-2.993819
H	0.514687	-2.007052	-5.185763
H	-2.378114	1.078042	-4.407229
H	-1.323852	1.529796	-2.255988
H	1.575329	-1.552235	2.993819
H	0.514687	-2.007052	5.185763
H	-2.378114	1.078042	4.407229
H	-1.323852	1.529796	2.255988
H	-2.877363	-0.557399	7.591579
H	-2.440663	0.938180	6.730543
H	-3.496309	-0.275986	5.946129
H	-2.877363	-0.557399	-7.591579
H	-3.496309	-0.275986	-5.946129
H	-2.440663	0.938180	-6.730543

--link1--

wB97XD/6-311+G* Int(Grid=UltraFine)
SCRF=(PCM,Solvent=Acetonitrile)

Cation 2a(+), wB97X-D/6-311+G* structure (C2v) in acetonitrile

1,2

C	0.000000	2.721812	-1.185562
C	0.000000	2.543755	0.222301
C	0.000000	3.689140	1.067057
C	0.000000	4.935851	0.524847
C	0.000000	5.106810	-0.884087
C	0.000000	3.977079	-1.730158
N	0.000000	1.279385	0.759010
B	0.000000	0.000000	-0.177411
F	1.152295	0.000000	-0.937990
O	0.000000	6.351047	-1.304416
C	0.000000	6.641775	-2.708259
N	0.000000	1.207844	2.061712
C	0.000000	0.000000	2.615682
C	0.000000	0.000000	4.056111
N	0.000000	0.000000	5.205648
N	0.000000	-1.207844	2.061712
N	0.000000	-1.279385	0.759010
C	0.000000	-2.543755	0.222301
C	0.000000	-3.689140	1.067057
C	0.000000	-4.935851	0.524847
C	0.000000	-5.106810	-0.884087
C	0.000000	-3.977079	-1.730158
C	0.000000	-2.721812	-1.185562
O	0.000000	-6.351047	-1.304416
C	0.000000	-6.641775	-2.708259
F	-1.152295	0.000000	-0.937990
H	0.000000	-3.561353	2.139818
H	0.000000	-5.818920	1.151524
H	0.000000	-4.085453	-2.805796
H	0.000000	-1.871295	-1.850543
H	0.000000	3.561353	2.139818
H	0.000000	5.818920	1.151524
H	0.000000	4.085453	-2.805796
H	0.000000	1.871295	-1.850543
H	0.000000	7.725173	-2.775556
H	0.897852	6.238627	-3.177856
H	-0.897852	6.238627	-3.177856
H	0.000000	-7.725173	-2.775556
H	-0.897852	-6.238627	-3.177856
H	0.897852	-6.238627	-3.177856

--link1--

wB97XD/6-311+G* Int(Grid=UltraFine)
SCRF=(PCM,Solvent=Acetonitrile)

Dication 2a(2+), wB97X-D/6-311+G* structure (C2v) in
acetonitrile

2,1

C	0.000000	2.702084	-1.211973
C	0.000000	2.520802	0.224417
C	0.000000	3.684829	1.085456
C	0.000000	4.917306	0.548872
C	0.000000	5.081888	-0.879862
C	0.000000	3.941329	-1.746522
N	0.000000	1.298640	0.745387
B	0.000000	0.000000	-0.201669
F	1.155242	0.000000	-0.933120
O	0.000000	6.295330	-1.289998
C	0.000000	6.639856	-2.697346
N	0.000000	1.215835	2.066590
C	0.000000	0.000000	2.589081
C	0.000000	0.000000	4.036060
N	0.000000	0.000000	5.184343
N	0.000000	-1.215835	2.066590
N	0.000000	-1.298640	0.745387
C	0.000000	-2.520802	0.224417
C	0.000000	-3.684829	1.085456
C	0.000000	-4.917306	0.548872
C	0.000000	-5.081888	-0.879862
C	0.000000	-3.941329	-1.746522
C	0.000000	-2.702084	-1.211973
O	0.000000	-6.295330	-1.289998
C	0.000000	-6.639856	-2.697346
F	-1.155242	0.000000	-0.933120
H	0.000000	-3.543558	2.156084
H	0.000000	-5.808499	1.162702
H	0.000000	-4.065872	-2.819930
H	0.000000	-1.849431	-1.873707
H	0.000000	3.543558	2.156084
H	0.000000	5.808499	1.162702
H	0.000000	4.065872	-2.819930
H	0.000000	1.849431	-1.873707
H	0.000000	7.723728	-2.713011
H	0.901139	6.249318	-3.166312
H	-0.901139	6.249318	-3.166312
H	0.000000	-7.723728	-2.713011
H	-0.901139	-6.249318	-3.166312
H	0.901139	-6.249318	-3.166312

References

1. S. M. Barbon, P. A. Reinkeluers, J. T. Price, V. N. Staroverov and J. B. Gilroy, *Chem. Eur. J.*, 2014, **20**, 11340–11344.
2. N. G. Connelly and W. E. Geiger, *Chem. Rev.*, 1996, **96**, 877–910.
3. W. Miao, J.-P. Choi and A. J. Bard, *J. Am. Chem. Soc.*, 2002, **124**, 14478–14485.
4. T. J. Stockmann and Z. Ding, *Can. J. Chem.*, 2015, **93**, 13–21.
5. A. J. Bard and L. R. Faulkner, *Electrochemical Methods: Fundamentals and Applications*, Wiley, New York, ed. 2, 2001.
6. *Gaussian 09*, Revision D.01, M. J. Frisch, G. W. Trucks, H. B. Schlegel, G. E. Scuseria, M. A. Robb, J. R. Cheeseman, G. Scalmani, V. Barone, B. Mennucci, G. A. Petersson, H. Nakatsuji, M. Caricato, X. Li, H. P. Hratchian, A. F. Izmaylov, J. Bloino, G. Zheng, J. L. Sonnenberg, M. Hada, M. Ehara, K. Toyota, R. Fukuda, J. Hasegawa, M. Ishida, T. Nakajima, Y. Honda, O. Kitao, H. Nakai, T. Vreven, J. A. Montgomery, Jr., J. E. Peralta, F. Ogliaro, M. Bearpark, J. J. Heyd, E. Brothers, K. N. Kudin, V. N. Staroverov, T. Keith, R. Kobayashi, J. Normand, K. Raghavachari, A. Rendell, J. C. Burant, S. S. Iyengar, J. Tomasi, M. Cossi, N. Rega, J. M. Millam, M. Klene, J. E. Knox, J. B. Cross, V. Bakken, C. Adamo, J. Jaramillo, R. Gomperts, R. E. Stratmann, O. Yazyev, A. J. Austin, R. Cammi, C. Pomelli, J. W. Ochterski, R. L. Martin, K. Morokuma, V. G. Zakrzewski, G. A. Voth, P. Salvador, J. J. Dannenberg, S. Dapprich, A. D. Daniels, O. Farkas, J. B. Foresman, J. V. Ortiz, J. Cioslowski, and D. J. Fox, Gaussian, Inc., Wallingford CT, 2013.
7. J.-D. Chai and M. Head-Gordon, *Phys. Chem. Chem. Phys.*, 2008, **10**, 6615–6620.